Full Length Article

Impact of orientation of blast initiation on ground vibrations

Dayamoy Garai [a], Hemant Agrawal [b,*], Arvind Kumar Mishra [a]

[a] *Indian Institute of Technology (ISM), Dhanbad, India*
[b] *Central Mine Planning and Design Institute Limited, Ranchi, India*

ARTICLE INFO

ABSTRACT

The blast-induced ground vibrations can be significantly controlled by varying the location and orientation of point of interest from blast site. The blast waves generated due to individual holes get superimposed and resultant peak particle velocity (PPV) generates. With the orientation sequence of holes blasts on site, the superimposition angle of wave changes and hence results in significant variation in resultant PPV. The orientation with respect to the initiation of blasts resulting in lowest PPV needs to be identified for any site. By knowing the PPV contour of vibration waves in mine sites, it is possible to reduce the vibration on the structures by changing the initiation sequence. In this paper, experimental blasts were conducted at two different mine sites and the PPV values were recorded at different orientations from the blast site and its initiation sequence. The PPV contours were drawn to identify the orientation with least and highest PPV generation line. It was found that by merely changing the initiation sequence of blasts with respect to the sensitive structure or point of interest, the PPV values can be reduced significantly up to 76.9%.

1. Introduction

Blast-induced ground vibration in and around mines has become a serious environmental issue. From the perspective of mining industry, it is a critical issue which needs to be properly addressed. With restrictions being increasingly imposed by local councils, vibration monitoring has become an essential part of the mine operation (Garai et al., 2018a; Norén-Cosgriff et al., 2020). Blasting is the principal method of rock breakage in mining throughout the world. This may be due to distinct advantages such as economy, efficiency, convenience and ability to break the hardest rocks. However, only a portion of the total energy of the explosive is consumed in breaking rocks while the rest is dissipated (Allsman, 1960; Hamdi et al., 2008; Agrawal and Mishra, 2018a). The mining and explosives industries are embracing new technology rapidly in order to improve overall performance, efficiency, and cost effectiveness in various types of blasting to mitigate its adverse effects (Agrawal and Mishra, 2018b; Mishra et al., 2019; Sharma et al., 2021a). Most recent technologies to reduce the adverse effects of explosives and blasting are precise in delay timing using electronic detonators system (Siskind et al., 1980; Agrawal and Mishra, 2017; Silva et al., 2018). Flexible timing allows blasters to make small hole to hole and row to row changes to account for drilling inaccuracies. With increasing mining activities in areas close to human settlements, ground vibration has induced environmental and social impacts as it can cause human annoyance and structure damages (Siskind et al., 1980). It has become imperative to measure and control the environmentally sensitive parameters of blasting (Dick, 1968; Mishra, 2013; Ziaran et al., 2013). The challenge for blasting engineers is the optimization of the blasts fragmentation and vibration levels in terms of its peak particle velocity (PPV) and frequency (Devine, 1966; Sanchidrián et al., 2007; Singh et al., 2016, 2021; Garai et al., 2018b). Numerous techniques and control methods have been suggested for controlling blast-induced ground vibrations (e.g. Singh et al., 2006; Shi and Chen, 2011; Ainalis et al., 2017; Agrawal and Mishra, 2019; Zhou et al., 2020). The blasting design and sequencing of blasting hole by providing the delay between holes is one of the important steps to maximize the utilization of the explosive energy and minimize ground vibrations (Singh et al., 2019, 2020; Roy et al., 2020). The accuracy in detonation of each hole at designated time as per blasting design helps in non-overlapping of holes (Agrawal and Mishra, 2020a). The blast-induced ground vibration may damage the sensitive structures nearby the mines (Liang et al., 2011; Nateghi, 2011; Sharma et al., 2021b).

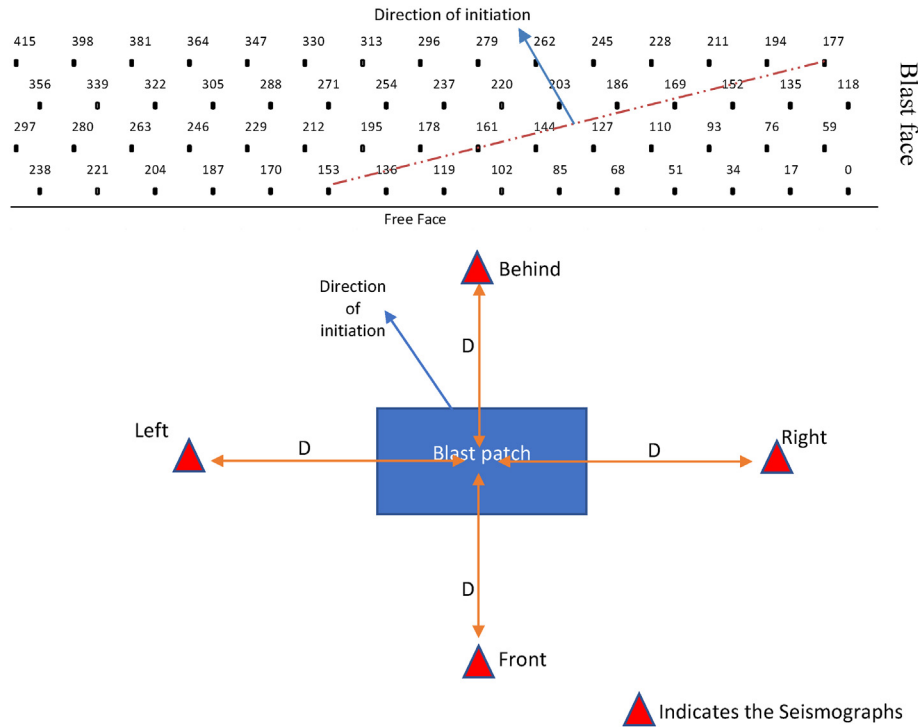https://doi.org/10.1016/j.jrmge.2022.03.012

Fig. 1. A general blasting patch and its vibration monitoring setup during experimental blasts conducted at opencast mines.

Recently, various studies are focused on prediction of the ground vibration using different artificial intelligence tools in terms to blasting design parameters. Different numerical methods such as artificial neural network, convolution neural network (Rezaeineshat et al., 2020), support vector machine (Hasanipanah et al., 2015; Bi et al., 2019), adaptive neuro-fuzzy interface system (Singh et al., 2008), random forest (Zhou et al., 2020; Kumar and MishraChoudhary, 2021), Monte Carlo technique (Little and Blair, 2010; Silva et al., 2018) have been used to predict blast-induced ground vibration. Although numerical methods may help in prediction of blast vibration, blast designing knowledge is essential.

The distance between the blast site and sensitive structure or point of interest is fixed. The increasing level of accuracy and better understanding of blasting mechanism show the importance of shock wave and its superimposition in PPV generation (Zhang and Naarttijärvi, 2005; Chu et al., 2018; Jayasinghe et al., 2019; Agrawal and Mishra, 2020b). The better understanding of the behavior of superimposition of shock wave during blasting will give blasting engineers opportunities to reduce ground vibrations (Nicholls et al., 1971; Müller et al., 2007; Singh et al., 2020). If superimposition behavior is known, the orientation of structure with respect to blast sequence may vary to minimize the PPV over the structures. It is important to know the orientation with respect to initiation sequence where the vibration is minimum in the particular mine geology.

The study was conducted at two opencast mines to evaluate the effect of orientation with respect to initiation sequence on the magnitude of blast-induced ground vibrations. The instrumentation was done at the site with respect to the point of initiation and free face. The magnitude of vibration in all four orientations were monitored and recorded with the help of instruments, keeping the inter hole and inter row delay the same for every blasting. The explosive charge was also varied to understand the change in magnitude of the ground vibration levels that can affect the structures present near to the blasting area.

2. Methods

The blasts were conducted at two different opencast coal mines with varying maximum charge per delay (MCPD). The blast-induced ground vibration was monitored at four orientations (left, right, front and behind the blast patch) with respect to initiation sequence, as presented in Fig. 1. The PPV values were plotted on a contour plot against its scaled distance (SD). The pattern of vibration wave superimposition and resultant PPV were then identified. The orientation at which the minimum and maximum PPV values were found has been obtained.

3. Experiment site details

Two opencast coal mines were chosen to perform the experimental blasts and vibration monitoring. The two mines are Giddi-C opencast coal mine of Central Coalfields Limited (CCL) – A subsidiary Coal India Limited, and Belpahar opencast coal mine of Mahandi Coalfields Limited (MCL) – A subsidiary Coal India Limited.

3.1. Giddi-C opencast coal project (OCP), CCL

Giddi–C is a part of South Karnapura coalfields situated in Ramgarh district (Jharkhand) and lies between latitude 23°24′21″N and 23°43′00″N and longitude 85°20′25″E and 85°25′00″E, and at an altitude of 378 m above mean sea level. The project is under the administrative control of CCL's Argada area (Fig. 2).

Giddi–C is connected with Ramgarh by motorable roads both via Sirka and Gidi-A Collieries. It is situated at a distance of 25 km from Ramgarh via Sirka colliery. The Patratu Saunda branch line of eastern railway extends to the middle of the property.

Overburden (OB) is being removed by shovel dumper combination. Gradient of the coal seam is 1: 2.86. Stripping ratio of Giddi-

Fig. 2. Satellite view of Giddi-C OCP, CCL (Red line indicating the cutting edge of the mine) (Source: Google Maps).

Fig. 4. Satellite view of Belpahar OCP, MCL (Orange line indicating the cutting edge of the mine (Source: Google Maps).

C OCP presently is 1:1.39. Giddi-C OCP is being mined by the opencast mining method using various combinations of Heavy Earth Moving Machineries (HEMMs) depending upon the seam parameters and the parting in between the coal seams.

A total of 15 blasts were conducted in Giddi-C OCP. The vibration has been recorded in all four directions i.e. front, back, left and right for 15 different blasts as indicated using 4 seismographs from distance of 60−250 m. The blasts were varied from 30 to 70 holes keeping the spacing and burden constant, i.e. 4.5 m and 4 m, respectively. The MCPD varied from 45 kg to 55 kg. The blasts were conducted using electronic detonators for precise initiation of each hole as per the blast hole sequencing pattern. The blast design and initiation pattern used in Giddi-C project is presented in Fig. 3.

3.2. Belpahar OCP, MCL

Belpahar OCP is situated in the IB Valley coalfields in Jharshuguda district of Orissa. The mine is situated between 21°42′20"N to 21°47′00"N and 83°49′35"E to 83°53′00"E. Belpahar opencast project is 12 km south from both Belpahar and Brajarajnagar railway stations. Mine area is bounded at south-side by Kushraloi village and at north-west side by Odisha Power Generation Corporation (OPGC) railway station line. Towards east, it is bounded by the Kirarama and Bandhbahal villages (Fig. 4).

The strike of the strata is slightly curvilinear, and the general trend being north-south. The strike changes to NE-SW in the north and again swings to NW-SE in the south. The dip is 4°−6° i.e. 1 in 10 to 1 in 14.

A total of 17 blasts were conducted in Belpahar OCP. The vibration has been recorded in all four directions i.e. front, back, left and right for 17 different blats as indicated using 4 seismographs from distance 50−270 m. The blasts were varied from 40 to 90 holes keeping the spacing and burden constant, i.e. 4.5 m and 4 m, respectively. The MCPD varied from 45 kg to 55 kg. The blast design and initiation pattern used in Belpahar OCP is presented in Fig. 5.

4. Data analysis

As discussed above, the blast vibrations generated due to blasting were recorded at four mutually perpendicular orientations, as presented in Fig. 1. A total number of 32 blasts were conducted, of which 15 blasts were conducted at Giddi-C and 17 blasts were conducted at Belpahar. The total 60 and 68 vibration events were recorded at Giddi-C and Belpahar, respectively. The summary of blasts conducted at Giddi-C and Belpahar has been tabulated in Table 1.

The blasts were conducted using different charges in holes and total charge of blasts. The details of blasts conducted in Giddi-C and Belpahar OCP are presented in Tables 2 and 3, respectively.

The PPV data collected at Giddi-C OCP have been plotted against its SD to observe the vibration variation with orientation. The SD curve has been plotted separately for each orientation with both mines datasets. The best fitted SD equation suggested by United Stated Bureau of Mines (USBM) has been extracted using regression. Figs. 6 and 7 present the PPV vs SD curve for Giddi-C OCP and Belpahar OCP, respectively.

The SD equations of each orientation have been extracted and compared to see the average variation/difference of PPV orientation. Eqs. (1)–(4) obtained from Fig. 4 at Giddi-C mine have been presented. It is noted that the maximum PPV values were recorded behind the face of blasts and the minimum PPV values were recorded in front of the blasts.

$$PPV = 247.09SD^{-1.08} \text{ (Behind the face)} \tag{1}$$

$$PPV = 437.63SD^{-1.437} \text{ (Left side of the face, } -22.15\%) \tag{2}$$

$$PPV = 257.57SD^{-1.321} \text{ (Right side of face, } -40.15\%) \tag{3}$$

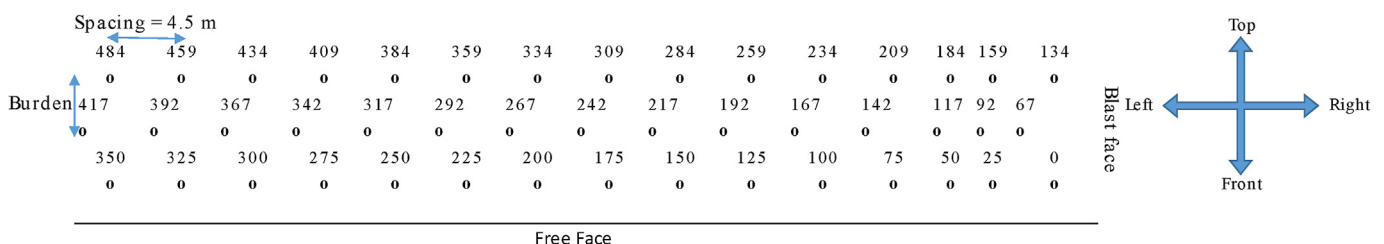$$PPV = 182.82SD^{-1.397} \text{ (In front of the face, } -64.34\%) \tag{4}$$

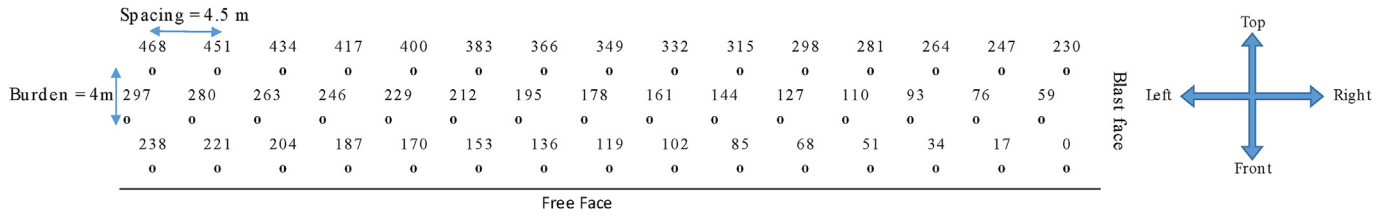**Fig. 3.** General blast hole sequencing pattern adopted at Giddi-C project.

Fig. 5. General blast hole sequencing pattern adopted at Giddi-C OCP.

Table 1
Summary of blasts conducted at Giddi-C OCP and Belpahar OCP.

Parameters of blasts	Giddi-C	Belpahar
Number of blasts	15	17
Number of vibration events	60	68
Number of holes.	30–70 holes	40–90 holes
MCPD (kg)	45–55	45–55
Diameter of hole (mm)	160	160
Spacing (m)	4.5	4.5
Burden (m)	4	4
Distance of vibration events (m)	60–250	50–270

From Eqs. (1)–(4), it has been found that there is an average reduction of PPV by 22.15% in left orientation (see Figs. 1), 40.15% in right orientation and 64.34% in front of the face with respect to behind the face PPV records at Giddi-C mine.

Similarly, Eqs. (5)–(8) obtained from Fig. 5 at Belpahar mine have been presented. Again, it has been observed that the maximum PPV values were recorded behind the face of blasts and the minimum PPV values were recorded in front of the blasts.

$$PPV = 668.96SD^{-1.446} \text{ (Behind the face)} \tag{5}$$

Table 2
Details of blasts design, recorded PPV and explosive charge of the blasts conducted at Giddi-C OCP.

No.	Number of holes	Hole diameter (mm)	Parameters (m)			Explosive charge (kg)			Distance (m)				PPV (mm/s)			
			Depth	Burden (B)	Spacing (S)	Per hole	Q_{max}/delay	Per Round	Behind the face	Left side of face	Right side of face	In front of face	Behind the face	Left side of face	Right side of face	In front of face
1	30	160	6.1–6.3	4	4.5	50.15	50.15	1504.5	60	60	60	60	23.82	18.69	17.66	8.73
2	45	160	6.2–6.3	4	4.5	55.15	55.15	2481.75	120	120	120	120	14.41	9.692	7.562	5.02
3	56	160	6.0–6.2	4	4.5	50.15	50.15	2808.4	90	90	90	90	16.19	13.26	10.03	6.72
4	40	160	6.1–6.4	4	4.5	55.15	55.15	2206	110	110	110	110	15.85	9.863	7.728	4.23
5	60	160	6.0–6.3	4	4.5	50.15	50.15	3009	100	100	100	100	15.91	10.97	7.377	4.77
6	55	160	5.9–6.2	4	4.5	50.15	50.15	2758.25	150	150	150	150	8.932	6.742	6.248	3.012
7	50	160	5.9–6.1	4	4.5	45.15	45.15	2257.5	230	230	230	230	5.694	2.421	2.558	1.271
8	47	160	6.0–6.2	4	4.5	50.15	50.15	2357.05	170	170	170	170	8.025	4.094	3.816	2.275
9	53	160	6.1–6.2	4	4.5	55.15	55.15	2922.95	130	130	130	130	9.125	4.596	3.504	2.355
10	50	160	6.0–6.3	4	4.5	55.15	55.15	2757.5	160	160	160	160	8.172	4.851	4.321	2.837
11	55	160	6.1–6.2	4	4.5	50.15	50.15	2758.25	120	120	120	120	9.75	4.596	3.504	2.355
12	48	160	6.0–6.1	4	4.5	50.15	50.15	2407.2	155	155	155	155	8.083	5.51	4.213	1.978
13	35	160	6.1–6.3	4	4.5	55.15	55.15	1930.25	210	210	210	210	6.751	3.061	2.373	1.95
14	70	160	6.0–6.2	4	4.5	50.15	50.15	3510.5	200	200	200	200	7.456	4.999	4.351	1.699
15	50	160	6.1–6.3	4	4.5	55.15	55.15	2757.5	140	140	140	140	10.256	8.941	7.338	2.075

Table 3
Details of blasts design, recorded PPV and explosive charge of the blasts conducted at Belpahar OCP.

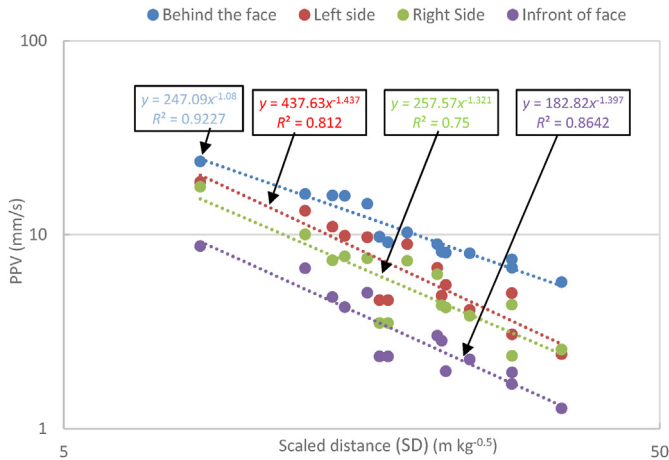| No.	Number of holes	Hole diameter (mm)	Parameters (m)			Explosive charge (kg)			Distance (m)				PPV (mm/s)			
			Depth	Burden (B)	Spacing (S)	Per hole	Q_{max}/delay	Per Round	Behind the face	Left side of face	Right side of face	In front of face	Behind the face	Left side of face	Right side of face	In front of face
1	70	160	6.0–6.2	4	4.5	55.1	55.1	3857	260	260	260	260	2.62	2.315	2.236	1.839
2	80	160	6.1–6.2	4	4.5	55.1	55.1	4408	275	275	275	275	2.332	1.763	1.507	1.366
3	75	160	5.9–6.1	4	4.5	50.1	50.1	3757.5	180	180	180	180	8.026	2.219	2.168	1.83
4	60	160	6.0–6.3	4	4.5	55.1	55.1	3306	150	150	150	150	12.58	10.98	10.54	3.299
5	58	160	5.8–6.1	4	4.5	50.1	50.1	2905.8	200	200	200	200	5.224	3.993	3.431	2.392
6	67	160	6.0–6.3	4	4.5	55.1	55.1	3691.7	75	75	75	75	16.75	15.45	12.95	9.814
7	60	160	5.9–6.1	4	4.5	50.1	50.1	3006	50	50	50	50	38.45	21.18	16.49	13.68
8	40	160	6.0–6.2	4	4.5	55.1	55.1	2204	60	60	60	60	29.31	21.91	21.77	9.25
9	56	160	6.1–6.3	4	4.5	55.1	55.1	3085.6	130	130	130	130	12.46	7.126	6.191	3.216
10	75	160	6.0–6.2	4	4.5	55.1	55.1	4132.5	160	160	160	160	10.232	5.239	5.03	4.22
11	50	160	6.1–6.2	4	4.5	55.1	55.1	2755	70	70	70	70	25.97	21.76	20.38	8.068
12	62	160	5.8–6.2	4	4.5	50.1	50.1	3106.2	220	220	220	220	5.021	2.362	2.629	1.649
13	50	160	5.9–6.1	4	4.5	50.1	50.1	2505	190	190	190	190	6.732	3.578	3.243	2.533
14	45	160	6.0–6.2	4	4.5	55.1	55.1	2479.5	75	75	75	75	25.75	15.57	15.42	8.739
15	90	160	6.1–6.3	4	4.5	55.1	55.1	4959	150	150	150	150	10.68	7.935	7.585	5.213
16	80	160	6.0–6.1	4	4.5	55.1	55.1	4408	200	200	200	200	5.374	3.514	3.38	2.321
17	75	160	6.0–6.2	4	4.5	55.1	55.1	4132.5	100	100	100	100	13.13	10.27	7.655	4.325

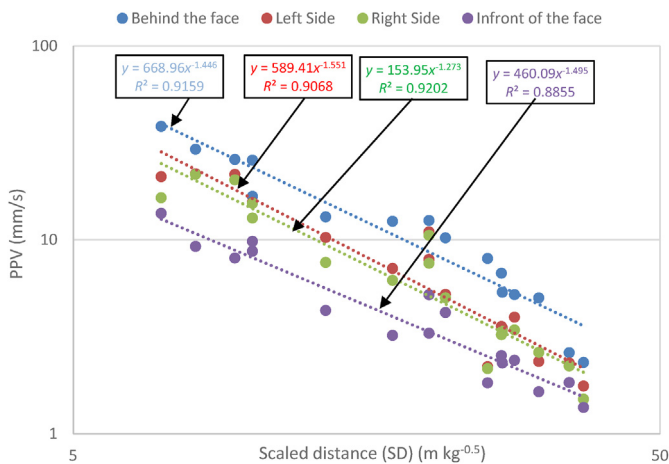**Fig. 6.** Plot showing PPV vs SD for data recorded at Giddi-C OCP, CCL.

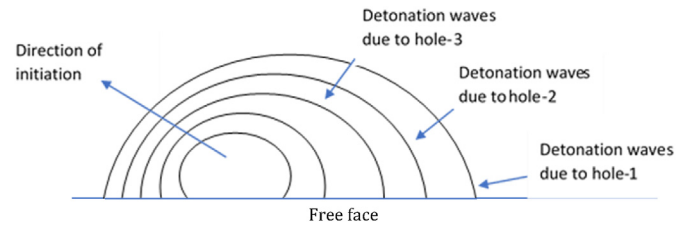**Fig. 7.** Plot showing PPV vs. SD for data recorded at Belpahar OCP, MCL.

Fig. 9. A general presentation of shock wave propagation during blasting.

$$PPV = 589.41SD^{-1.551} \text{ (Left side of the face, } -11.9\%) \qquad (6)$$

$$PPV = 460.09SD^{-1.495} \text{ (Right side of face, } -31.22\%) \qquad (7)$$

$$PPV = 153.95SD^{-1.273} \text{ (In front of the face, } -76.9\%) \qquad (8)$$

From Eqs. (5)—(8), it has been found that there is an average reduction of PPV by 11.9% in left orientation (see Figs. 1), 31.22), 31.22% in right orientation, and 76.9% in front of the face with respect to behind the face PPV records at Belpahar mine.

5. Contour analysis

The data recorded at two different mines were further plotted against the SD on a contour mapping. Fig. 8 presents the comparison of contour mapping of PPV against its SD plotted for Giddi-C and Belpaharv OCP. The orientation at which the highest PPV values were recorded is shown with a red arrow in the figure. The highest PPV line coincides with the initiation orientation, which is also true as per the concept of wave superimposition. In both the cases, the minimum PPV values found to be in front of face as free face reflected the shock wave generated due to blasting.

In Fig. 8, at both the mines with different local geological conditions and different blast design parameters (as summarized in Table 1), the highest PPV is recorded along the initiation orientation which propagates to larger SD. Moreover, it has been observed that
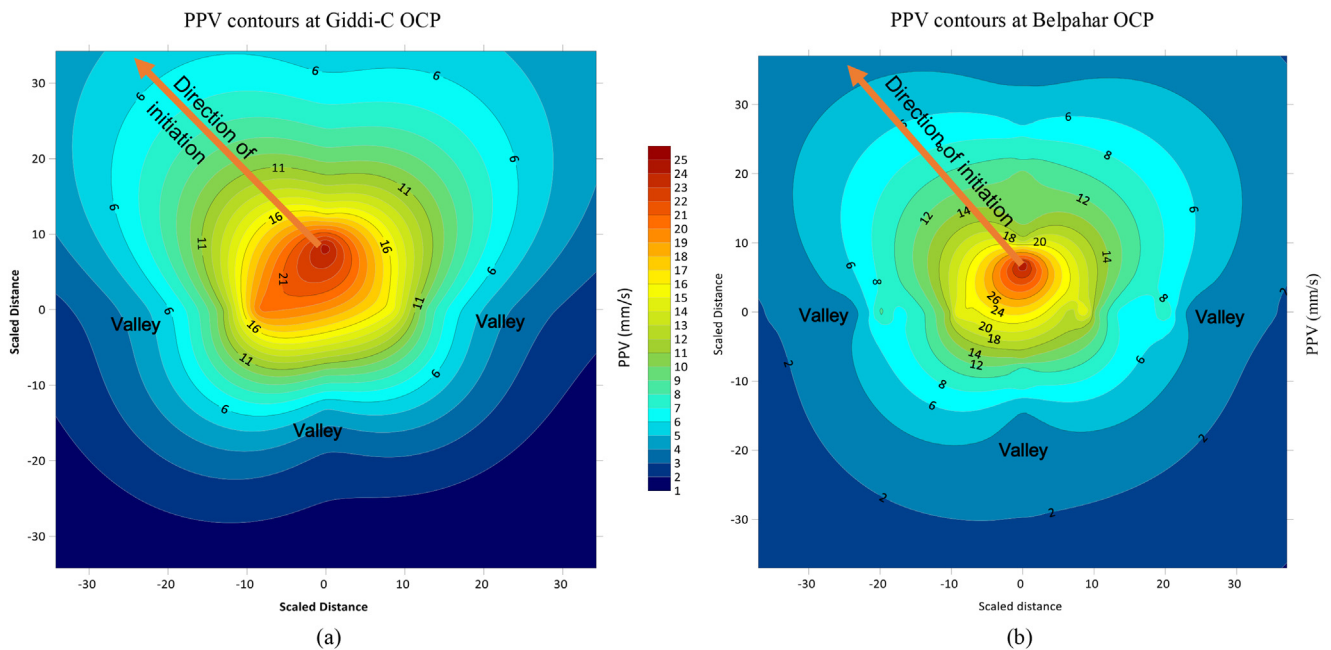

Fig. 8. Comparison of PPV contours at (a) Giddi-C and (b) Belpahar OCP.

in both the contour maps, the lowest PPV is recorded in front of the blasts, which propagates to a shorter SD. In both the mine sites, the contour maps show steep valleys in the left and right sides parallel to the blast site, i.e. the center point of the map and in front side, and further an increasing dome is noticed as we move behind the face. This may be due higher superimposition in the initiation orientation which is behind the face.

6. Discussion

The PPV values were recorded at all mutual perpendicular orientations from the face, and the SD equation and PPV contours of both mines have been obtained. It was found that the minimum PPV values were obtained in front of the face, and maximum PPV values were obtained along the initiation orientation of holes. By changing the initiation sequence/initiation orientation of blasts with respect to the sensitive structure or point of interest, the PPV values can be significantly changed to 76.9% (see Eq. (8)). The observations are evident and also match with the concept of wave superimpositions. Along the sequence orientation of holes, the wave superimposition will be highest, whereas in front of blasting face, the PPV values will be lowest due to reflection of waves from the free face. Fig. 8 presents the ideal shock wave generation due to each blast hole and its propagation along the ground. Fig. 9 presents that the highest chances of constructive superimposition of shock waves are at the initiation orientation and hence highest PPV values. While, in front of the blasting face, the free face which will reflect the waves and propagation of shock waves will be minimum.

This concept of variation of PPV due to wave superimposition can be utilized to avoid the highest line of PPV to be aligned along the sensitive structure. Although the results may change if any major geological discontinuity or any other geological changes is presented in between the blasting point and point of PPV record. By adopting the contour mapping technique of PPV, the most probable line of highest PPV can be identified for a particular mine.

7. Conclusions

In this study, the impact of the initiation orientation of blast on ground vibrations has been discussed. The trial blasts were conducted at two different mines and vibration at four mutually perpendicular orientations has been recorded. The following conclusions have been obtained:

(1) The sensitive structure or point of interest should not be aligned along the initiation orientation of production blasts.
(2) The PPV contouring method helps in identification of the orientation of least and highest PPV generation lines. The PPV contour will also help in better understanding of ground vibration generation in the particular geology of any mine site.
(3) By merely changing the initiation sequence of blasts with respect to the sensitive structure or point of interest, the PPV values can be significantly reduced up to 76.9%.

Declaration of competing interest

The authors declare that they have no known competing financial interests or personal relationships that could have appeared to influence the work reported in this paper.

References

Agrawal, H., Mishra, A.K., 2017. Evolution of digital detonators as an intelligent tool for control blasting in Indian mines. Ann. Chimie Sci. Matériaux 41 (3–4), 157–171.

Agrawal, H., Mishra, A.K., 2018a. Evaluation of initiating system by measurement of seismic energy dissipation in surface blasting. Arabian J. Geosci. 11 (13), 345.

Agrawal, H., Mishra, A.K., 2018b. Probabilistic analysis on scattering effect of initiation systems and concept of modified charge per delay for prediction of blast induced ground vibrations. Measurement 130, 306–317.

Agrawal, H., Mishra, A.K., 2019. Modified scaled distance regression analysis approach for prediction of blast-induced ground vibration in multi-hole blasting. J. Rock Mech. Geotech. 11 (1), 202–207.

Agrawal, H., Mishra, A.K., 2020a. An innovative technique of simplified signature hole analysis for prediction of blast-induced ground vibration of multi-hole/production blast: an empirical analysis. Nat. Hazards 100 (1), 111–132.

Agrawal, H., Mishra, A.K., 2020b. An analytical approach to measure the probable overlapping of holes due to scattering in initiation system and its effect on blast-Induced ground vibration in surface mines. Min. Metall. Explor. 38, 485–495.

Ainalis, D., Olivier, K., Jean-Pierre, T., Olivier, V., Georges, K., 2017. Modelling the source of blasting for the numerical simulation of blast-induced ground vibrations: a review. Rock Mech. Rock Eng. 50 (1), 171–193.

Allsman, P.L., 1960. Analysis of explosive action in breaking rock. Inst. Min. Metall. Petrol. Eng. Trans. 217, 469–478.

Bi, L., Xie, W., Zhao, J.J., 2019. Automatic recognition and classification of multi-channel microseismic waveform based on DCNN and SVM. Comput. Geosci. 123, 111–120.

Chu, H.B., Yang, X.L., Li, S.J., Liang, W.M., 2018. Experimental investigation of the propagation and attenuation rule of blasting vibration wave parameters based on the damage accumulation effect. Shock Vib. 2018, 2493149.

Devine, J.F., 1966. Effect of Charge Weight on Vibration Levels from Quarry Blasting. US Department of the Interior, Bureau of Mines.

Dick, R.A., 1968. Factors in Selecting and Applying Commercial Explosives and Blasting Agents. US Department of the Interior, Bureau of Mines.

Garai, D., Agrawal, H., Mishra, A.K., Kumar, S., 2018a. Influence of initiation system on blast-induced ground vibration using random forest algorithm, artificial neural network, and scaled distance analysis. Math. Model. Eng. Probl. 5 (4), 418–426.

Garai, D., Mishra, A.K., Kumar, S., Agrawal, H., 2018b. Development of a universal blast-induced ground vibration prediction model for Jharia Coalfields. Modell., Meas. Control, C 79 (2), 46–55.

Hamdi, E., Romdhane, N.B., du Mouza, J., Le Cleac'h, J.M., 2008. Fragmentation energy in rock blasting. Geotech. Geol. Eng. 26 (2), 133–146.

Hasanipanah, M., Masoud, M., Shahnazar, A., Armaghani, D.J., Farazmand, A., 2015. Feasibility of indirect determination of blast induced ground vibration based on support vector machine. Measurement 75, 289–297.

Jayasinghe, B., Zhao, Z.Y., Chee, A.G.T., Zhou, H.Y., Gui, Y.L., 2019. Attenuation of rock blasting induced ground vibration in rock-soil interface. J. Rock Mech. Geotech. 11 (4), 770–778.

Kumar, S., Mishra, A.K., Choudhary, B.S., 2021. Prediction of Back Break in Blasting Using Random Decision Trees. Eng Comput. https://doi.org/10.1007/s00366-020-01280-9.

Liang, Q.G., An, Y.F., Zhao, L., Li, D.W., Yan, L.P., 2011. Comparative study on calculation methods of blasting vibration velocity. Rock Mech. Rock Eng. 44 (1), 93–101.

Little, T.N., Blair, D.P., 2010. Mechanistic Monte Carlo models for analysis of flyrock risk. Rock Frag. Blasting 9, 641–647.

Mishra, A.K., 2013. Unlocking possibility of blasting near residential structure using electronic detonators. J. Geol. Soc. India 81 (3), 429–435.

Mishra, A.K., Agrawal, H., Raut, M., 2019. Effect of aluminum content on detonation velocity and density of emulsion explosives. J. Mol. Model. 25 (3), 70–79.

Müller, B., Hausmann, J., Niedzwiedz, H., 2007. Comparison of different methods of measuring and calculating blast vibrations in rock masses. In: Proceeding of the 4th EFEE World Conference, Vienna.

Nateghi, R., 2011. Prediction of ground vibration level induced by blasting at different rock units. Int. J. Rock Mech. Min. Sci. 48 (6), 899–908.

Nicholls, H.R., Johnson, C.F., Duvall, W.I., 1971. Blasting Vibrations and Their Effects on Structures. US Government Printers, Washington, US.

Norén-Cosgriff, K.M., Ramstad, N., Neby, A., Madshus, C., 2020. Building damage due to vibration from rock blasting. Soil Dynam. Earthq. Eng. 138, 106331.

Rezaeineshat, A., Monjezi, M., Mehrdanesh, A., Khandelwal, M., 2020. Optimization of blasting design in open pit limestone mines with the aim of reducing ground vibration using robust techniques. Geomech. Geophys. Geo-Energy, Geo-Resour. 6 (2), 1–14.

Roy, M.P., Mishra, A.K., Agrawal, H., Singh, P.K., 2020. Blast vibration dependence on total explosives weight in open-pit blasting. Arabian J. Geosci. 13 (13), 1–8.

Sanchidrián, J.A., Segarra, P., López, L.M., 2007. Energy components in rock blasting. Int. J. Rock Mech. Min. Sci. 44 (1), 130–147.

Sharma, M., Agrawal, H., Choudhary, B.S., 2021a. Multivariate regression and genetic programming for prediction of backbreak in open-pit blasting. Neural Comput. Appl. 34, 2103–2114.

Sharma, M., Choudhary, B.S., Kumar, H., Agrawal, H., 2021b. Optimization of delay sequencing in multi-row blast using single hole blast concepts. J. Inst. Eng. 102, 453—460.

Shi, X.Z., Chen, S.H.R., 2011. Delay time optimization in blasting operations for mitigating the vibration-effects on final pit walls' stability. Soil Dynam. Earthq. Eng. 31 (8), 1154—1158.

Silva, J., Li, L.F., Gernand, J.M., 2018. Reliability analysis for mine blast performance based on delay type and firing time. Int. J. Min. Sci. Technol. 28 (2), 195—204.

Singh, T.N., Dontha, L.K., Bhardwaj, V., 2008. Study into blast vibration and frequency using ANFIS and MVRA. Min. Tech. 117 (3), 116—121.

Singh, P.K., Sirveiya, A.K., Babu, K.N., Roy, M.P., Singh, C.V., 2006. Evolution of effective charge weight per delay for prediction of ground vibrations generated from blasting in a limestone mine. Int. J. Min. Reclamat. Environ. 20 (1), 4—19.

Singh, P.K., Roy, M.P., Paswan, R.K., Sarim, Md, Kumar, S., Ranjan Jha, R., 2016. Rock fragmentation control in opencast blasting. J. Rock Mech. Geotech. Eng. 8 (2), 225—237.

Singh, C.P., Agrawal, H., Mishra, A.K., Singh, P.K., 2019. Reducing environmental hazards of blasting using electronic detonators in a large opencast coal project- a case study. J. Mine Met. Fuel 67 (7), 345—350.

Singh, C.P., Agrawal, H., Mishra, A.K., 2020. A study on influence of blast-induced ground vibration in dragline bench blasting using signature hole analysis. Arabian J. Geosci. 13 (13), 1—9.

Singh, C.P., Agrawal, H., Mishra, A.K., 2021. Frequency channeling: a concept to increase the frequency and control the PPV of blast-induced ground vibration waves in multi-hole blast in a surface mine. Bull. Eng. Geol. Environ. 80, 8009—8019.

Siskind, D.E., Strachura, V.J., Stagg, M.S., Kopp, J.W., 1980. Structure Response and Damage Produced by Airblast from Surface Mining. US Department of the Interior, Bureau of Mines.

Zhang, Z.X., Naarttijärvi, T., 2005. Reducing ground vibrations caused by underground blasts in LKAB Malmberget mine. Fragblast 9 (2), 61—78.

Zhou, J., Asteris, P.G., Armaghani, D.J., Pham, B.T., 2020. Prediction of ground vibration induced by blasting operations through the use of the Bayesian Network and random forest models. Soil Dynam. Earthq. Eng. 139, 106390.

Ziaran, S., Musil, M., Cekan, M., Chlebo, O., 2013. Analysis of seismic waves generated by blasting operations and their response on buildings. Int J. Environ. Eco. Eng. 7 (11), 501—506.

Dr. Hemant Agrawal received his B.tech, M.tech and PhD degrees in Mining Engineering from Indian School of Mines, Dhanbad, India. Presently, he is working as a Manager (Mining) at central mine planning and design institute Limited, Ranchi (A subsidiary company of Coal India Limited). His research interests include mine blasting, blast-induced ground vibration, controlled blasting technique, underground mining, initiation systems and opencast mining.